

Observation-centered Kalman filters

John T. Kent¹ and Shambo Bhattacharjee²
University of Leeds, Leeds, UK

Weston R. Faber³
L3Harris, Applied Defense Solutions, Colorado Springs, CO, USA

Islam I. Hussein⁴
L3Harris, Applied Defense Solutions, Herndon, VA, USA

Various methods have been proposed for the nonlinear filtering problem, including the extended Kalman filter (EKF), iterated extended Kalman filter (IEKF), unscented Kalman filter (UKF) and iterated unscented Kalman filter (IUKF). In this paper two new nonlinear Kalman filters are proposed and investigated, namely the observation-centered extended Kalman filter (OCEKF) and observation-centered unscented Kalman filter (OCUKF). Although the UKF and EKF are common default choices for nonlinear filtering, there are situations where they are bad choices. Examples are given where the EKF and UKF perform very poorly, and the IEKF and OCEKF perform well. In addition the IUKF and OCUKF are generally similar to the IEKF and OCEKF, and also perform well, though care is needed in the choice of tuning parameters when the observation error is small. The reasons for this behaviour are explored in detail.

I. Introduction

Consider a system of state and measurement (or observation) equations where (a) the propagation equation is linear, but (b) the measurement equation is nonlinear, and (c) the measurement

¹ Professor, Department of Statistics, j.t.kent@leeds.ac.uk.

² PhD student, Department of Statistics, mmsb@leeds.ac.uk.

³ Research Scientist, weston.faber@l3harris.com.

⁴ Senior R&D Scientist, islam.Hussein@l3harris.com.

or observation variance is small. Due to the nonlinearity, the classic Kalman filter (KF) is not defined, so various modifications have been proposed, including the extended Kalman filter (EKF), the iterated extended Kalman filter (IEKF), the unscented Kalman filter (UKF), and the iterated unscented Kalman filter (IUKF). To this collection two new filters are added here and given the names *observation-centered extended Kalman filter (OCEKF)* and *observation-centered unscented Kalman filter (OCUKF)*.

In this paper these filters are explored in a one-dimensional setting. In particular, it is shown that in certain circumstances with small measurement error,

- the EKF and UKF perform very poorly;
- the IEKF and OCEKF are similar to one another and perform well;
- the IUKF and OCUKF is generally similar to the IEKF and OCEKF, and also perform well, but if the measurement error is very small, care is needed in the choice of tuning parameters.

Although this paper is set in the context of a one-dimensional state and a one-dimensional observation, the ideas are also relevant in higher dimensions. An important example is given by the tracking problem in orbital dynamics. The state of an orbiting object is six-dimensional and an angles-only observation is two-dimensional. However, the main source of uncertainty in the state is often one-dimensional, given by the position of the object along the orbital path. The other five state variables do not change with time under Keplerian dynamics.

It is convenient to describe the position of the object along the orbital path using the *mean anomaly* because this choice makes the propagation equation linear. However, the projection of an angles-only observation onto the orbital plane is measured in terms of *true anomaly*. For a highly eccentric orbit the mapping between these two variables can be very nonlinear. A one-dimensional version of the tracking problem is studied in detail in Section V.

II. Background

A. The classic Kalman filter

Recall the classic Kalman filter [1], which is designed for linear propagation and observation equations, with Gaussian noise. There is a sequence of p -dimensional state vectors $\{\mathbf{x}_k\}$ and a

sequence of q -dimensional noisy (partial) observations $\{\mathbf{z}_k\}$ at times t_k , $k \geq 1$. Let \mathcal{F}_k denote the information contained in the first k observations $\mathbf{z}_1, \dots, \mathbf{z}_k$. The state vectors evolve through noisy linear propagation

$$\mathbf{x}_k = F_k \mathbf{x}_{k-1} + \mathbf{w}_k, \quad (\text{II.1})$$

where F_k is a $p \times p$ matrix and \mathbf{w}_k is system noise. The observations are noisy versions of linear functions of the state vectors,

$$\mathbf{z}_k = H_k \mathbf{x}_k + \mathbf{v}_k, \quad (\text{II.2})$$

where H_k is a $q \times p$ matrix and \mathbf{v}_k is measurement noise. The random vectors \mathbf{w}_k and \mathbf{v}_k are assumed independent of one another and of $\mathbf{z}_1, \dots, \mathbf{z}_{k-1}$, with $N_p(0, Q_k)$ and $N_q(0, R_k)$ distributions, respectively. The dimension p of the state vector is allowed to be different from the dimension q of the observation vector.

Start with an initial Gaussian distribution for \mathbf{x}_0 , with mean vector and covariance matrix denoted $\mathbf{x}_{0|0}, P_{0|0}$. Then the conditional propagated distribution of \mathbf{x}_k given \mathcal{F}_k , $k \geq 1$ follows a Gaussian distribution. The conditional mean vector and covariance matrix, denoted $\mathbf{x}_{k|k}, P_{k|k}$, say, can be determined iteratively as follows.

Suppose $\mathbf{x}_{k-1|k-1}$ and $P_{k-1|k-1}$ are known. After propagation from time t_{k-1} to t_k , the conditional distribution of the state becomes

$$\mathbf{x}_k | \mathcal{F}_{k-1} \sim N_p(\mathbf{x}_{k|k-1}, P_{k|k-1}),$$

where

$$\mathbf{x}_{k|k-1} = F_k \mathbf{x}_{k-1|k-1}, \quad P_{k|k-1} = F_k P_{k-1|k-1} F_k^T + Q_k.$$

Given the observation \mathbf{z}_k at time t_k the Bayesian update yields the posterior distribution

$$\mathbf{x}_k | \mathcal{F}_k \sim N(\mathbf{x}_{k|k}, P_{k|k})$$

with updated mean vector and covariance matrix

$$\mathbf{x}_{k|k} = \left(P_{k|k-1}^{-1} + H_k^T R_k^{-1} H_k \right)^{-1} \left(P_{k|k-1}^{-1} \mathbf{x}_{k|k-1} + H_k^T R_k^{-1} \mathbf{z}_k \right), \quad (\text{II.3})$$

$$P_{k|k} = \left(P_{k|k-1}^{-1} + H_k^T R_k^{-1} H_k \right)^{-1}. \quad (\text{II.4})$$

These expressions can also be written as

$$\begin{aligned}x_{k|k} &= x_{k|k-1} + K_k(z_k - H_k x_{k|k-1}) \\ P_{k|k} &= (I - K_k H_k) P_{k|k-1} (I - K_k H_k)^T + K_k R_k K_k^T,\end{aligned}$$

where

$$K_k = P_{k|k-1} H_k^T (H_k P_{k|k-1} H_k^T + R_k)^{-1}$$

B. The EKF, IEKF and OCEKF

The EKF was created to accommodate certain sorts of nonlinearity to generalize either F_k in the propagation equation or H_k in the observation equation. This paper is focused on the second situation in a very particular setting, namely

- the state and observation are one-dimensional, $p = q = 1$,
- the propagation equation is exactly linear as in (II.1), but
- the measurement equation is not linear so a generalization of (II.2) is needed.

The essential ingredients for one update step can be written in a more concise notation as follows:

$$x \sim N(\mu_x, \sigma^2) \tag{II.5}$$

$$z|x \sim N(h(x), \tau^2), \tag{II.6}$$

where $h(\cdot)$ is a known monotone function, and where x , μ_x , σ^2 , τ^2 correspond to x_k , $x_{k|k-1}$, $P_{k|k-1}$, R_k , respectively, in the previous section. The explicit conditioning on \mathcal{F}_{k-1} in the notation is dropped since everything is conditioned on it. Further, boldface is dropped since the vectors are scalars here. Also, it is possible to move back and forth between the state space and the observation space by writing $z(x) = h(x)$ for any x and $x(z) = h^{-1}(z)$ for any z .

Equation (II.5) can be regarded as a ‘‘prior’’ distribution for x , and (II.6) as the ‘‘likelihood’’ for the observation z given x . Hence the posterior distribution for x given a realization z_{obs} of the observation z is proportional to

$$f(x|z_{\text{obs}}) \propto \exp \left\{ -\frac{1}{2} \frac{(x - \mu_x)^2}{\sigma^2} - \frac{1}{2} \frac{(z_{\text{obs}} - h(x))^2}{\tau^2} \right\}. \tag{II.7}$$

The purpose of the update step in the EKF is to approximate this posterior distribution by a Gaussian distribution. Write

$$\begin{aligned} z_{\text{obs}} - h(x) &= z_{\text{obs}} - h(y) + h(y) - h(x) \\ &\approx z_{\text{obs}} - h(y) + h'(y)(y - x), \end{aligned} \quad (\text{II.8})$$

using a first order Taylor series expansion, where the choice of y is discussed below. Then the exponent in (II.7) becomes a quadratic function of x ; hence the approximating posterior distribution is Gaussian with mean and variance

$$\mu_{x|z_{\text{obs}}} = \mu_x + \frac{h'\sigma^2}{h'^2\sigma^2 + \tau^2} \{z_{\text{obs}} - h(y) + h'[y - \mu_x]\}, \quad (\text{II.9})$$

$$\sigma_{x|z_{\text{obs}}}^2 = \left(\frac{1}{\sigma^2} + \frac{h'^2}{\tau^2} \right)^{-1}, \quad (\text{II.10})$$

where $h' = h'(y)$.

There are three important choices for y .

(a) $y = \mu_x$, the prior mean. This choice gives the standard EKF [2, 3]. Equation (II.9) for the posterior mean simplifies to

$$\mu_{x|z_{\text{obs}}} = \mu_x + \frac{h'\sigma^2}{h'^2\sigma^2 + \tau^2} \{z_{\text{obs}} - h(\mu_x)\}. \quad (\text{II.11})$$

(b) $y = \mu_{x|z_{\text{obs}}}$, the posterior mean. This choice gives the iterated EKF [2]. Equation (II.9) for the posterior mean becomes

$$\mu_{x|z_{\text{obs}}} = \mu_x + \frac{h'\sigma^2}{h'^2\sigma^2 + \tau^2} \{z_{\text{obs}} - h(\mu_{x|z_{\text{obs}}}) + h'[\mu_{x|z_{\text{obs}}} - \mu_x]\}. \quad (\text{II.12})$$

Note that $\mu_{x|z_{\text{obs}}}$ occurs on both sides of the equation. Hence an iterative algorithm is needed to compute it.

(c) $y = x_{\text{obs}} = h^{-1}(z_{\text{obs}})$, the transformed observation. This choice gives the new proposal of this paper, the observation-centered EKF. Equation (II.9) for the posterior mean simplifies to

$$\mu_{x|z_{\text{obs}}} = \mu_x + \frac{h'\sigma^2}{h'^2\sigma^2 + \tau^2} \{x_{\text{obs}} - \mu_x\}. \quad (\text{II.13})$$

C. The UKF, IUKF and OCUKF

Various unscented filters (UKF, IUKF and OCUKF) can be defined as discrete approximations to the extended filters (EKF, IEKF and OCEKF). The starting point is a collection of three ‘‘sigma points’’

$$x_{-1} = y - \alpha\sigma, \quad x_0 = y, \quad x_1 = y + \alpha\sigma, \quad (\text{II.14})$$

where y is a centering point to be specified, and $\alpha > 0$ is a tuning parameter. Two sets of weights are defined,

$$\begin{aligned} w_{-1}^a = w_1^a &= \frac{1}{2\alpha^2}, & w_0^a &= 1 - \frac{1}{\alpha^2} \\ w_{-1}^c = w_1^c &= \frac{1}{2\alpha^2}, & w_0^c &= 1 - \frac{1}{\alpha^2} + 3 - \alpha^2. \end{aligned}$$

where the first weights are used to compute means and the second weights are used to compute variances and covariances.

The conventional choice of tuning parameter $\alpha = 0.001$ is used here so that the sigma points are close to y . The sigma points have weighted mean and variance.

$$\sum w_j^a x_j = y, \quad \sum w_j^c (x_j - y)^2 = \sigma^2,$$

where in all cases the sums range over $j = -1, 0, 1$.

Let $z_j = h(x_j)$ denote the transformed sigma points, with mean $\bar{z} = \sum w_j^a z_j$. Let $C = C(y)$ and $V = V(y)$ denote the weighted covariance between the $\{z_j\}$ and $\{x_j\}$, and the weighted variance of the $\{z_j\}$, respectively,

$$C(y) = \sum w_j^c (z_j - \bar{z})(x_j - y), \quad V(y) = \sum w_j^c (z_j - \bar{z})^2.$$

The limiting behavior of C, V and \bar{z} as $\alpha \rightarrow 0$ [4] is given by

$$V \rightarrow h'(y)^2 \sigma^2, \quad C \rightarrow h'(y) \sigma^2, \quad \bar{z} \rightarrow h(y) + \frac{1}{2} \sigma^2 h''(y). \quad (\text{II.15})$$

Hence several choices of unscented filter can be defined by mimicking the extended filters in (II.9)–(II.10),

$$\mu_{x|z_{\text{obs}}} = \mu_x + \frac{C}{V + \tau^2} \{z_{\text{obs}} - h(y) + (V/C)[y - \mu_x]\}, \quad \sigma_{x|z_{\text{obs}}}^2 = \sigma^2 - C^2/(V + \tau^2), \quad (\text{II.16})$$

for suitable values of y .

- (a) The standard UKF [5, 6] uses $y = \mu_x$. In addition it replaces $h(y)$ by \bar{z} in (II.16) to provide some bias correction.
- (b) The IUKF [7] uses $y = \mu_{x|z_{\text{obs}}}$ in (II.16). As conventionally formulated, the IUKF does not incorporate any bias correction.
- (c) Similarly to the IUKF, it is possible to define an observation centered UKF (OCUKF) by using $y = x_{\text{obs}} = h^{-1}(z_{\text{obs}})$ in (II.16).

III. Intuition behind the iterated and observation-centered filters

For an $N(\mu, \sigma^2)$ distribution, use the phrase *effective range* (or more precisely 95% effective range) to describe the interval $(\mu - 2\sigma, \mu + 2\sigma)$ covering 95% of the probability mass.

The Taylor series approximation in (II.8) will be a good approximation if h is approximately linear over an interval containing y and x . When τ^2 is small and σ^2 is not small, then the posterior distribution of x will be concentrated near x_{obs} . The choice $y = \mu_x$ may not be a good choice in this setting; the effective support of the posterior distribution of x may be a long way from μ_x and h may be very nonlinear over this interval. On the other hand, both $y = \mu_{x|z_{\text{obs}}}$ and $y = x_{\text{obs}}$ may be very good choices; these two values will be close together and the posterior distribution will be concentrated near both these choices.

More generally in the one-dimensional non-linear filtering system, information can be represented on two scales: the *signal scale* x and the *measurement or observation scale* z . The state variance σ^2 is on the signal scale and the observation variance τ^2 is on the measurement scale. Variability can be mapped back and forth between the two scales by assuming h is approximately linear over an appropriate range and multiplying or dividing by $h'(\xi)$ where ξ is an appropriate value within the interval (on the signal scale) on which the signal varies.

Hence there are two choices for linearization: the first choice is to map the prior variability in x from the signal scale to the measurement scale, and then to combine the prior variability with the likelihood on the measurement scale. This is the approach effectively taken in the standard EKF and UKF, with the posterior density finally mapped back to the signal scale. However, although the prior distribution of x is exactly Gaussian on the signal scale, it may be very non-Gaussian when

transformed to the measurement scale when σ^2 is not small.

The second choice is to map the variability in z about $h(x)$ from the measurement scale to the signal scale. Because τ^2 is assumed small, this is a reasonable approach; it is the approach taken by the iterated and observation-centered filters.

There are several features in this setup that make the iterated and observation-centered filters feasible and effective.

- The prior distribution of the signal is exactly normal.
- The transformation function h is allowed to be highly nonlinear.
- But the standard deviation τ for the distribution of an observation z given x is small.
- The mapping between signal space and observation space is one to one. In particular it is possible to define x_{obs} , the value on the signal scale corresponding to the observation z_{obs} on the measurement scale.

IV. Idealized analytic examples

To illustrate the issues involved, consider an idealized version of the problem and limit attention to the extended filters. Suppose $h(x) = x^\lambda$ is the mapping from the signal scale to the measurement scale, where λ is a known power. Let $\mu_x = 1$ and let $\tau^2 = 0$, so there is no measurement error. The choice of σ^2 is irrelevant for this section. Let $z_{\text{obs}} = 2$ be the realized value of the observation. Since $\tau^2 = 0$ the correct posterior distribution is concentrated at $\mu_{x|z} = h^{-1}(2) = 2^{1/\lambda}$.

The standard EKF gets the posterior variance $\sigma_{x|z_{\text{obs}}}^2 = 0$ correct, but gets the posterior mean wrong. Here are the details. For the standard EKF,

$$\mu_{x|z_{\text{obs}}} = 1 + 1/\lambda.$$

Results for standard EKF and IEKFs are summarized in Table 1. The table also includes the results for the observation-centered EKF, defined below. Note that the EKF overshoots the exact posterior mean if $\lambda > 1$ and undershoots the exact posterior mean if $\lambda < 1$. The IEKF and OCEKF results match the exact result.

Table 1 Comparison between various approximations to the posterior mean for the idealized example in Section IV. In each case the posterior variance is 0.

IEKF		
λ	EKF	OCEKF
Exact		
1	2	2.00
2	1.5	1.41
0.5	3	4

V. Application to 1d orbital dynamics

Consider a small body in orbit about a large body, such as a satellite about the earth. Suppose the object follows Keplerian dynamics, so that it follows an exact elliptical orbit. For simplicity suppose the orbital plane, the angle of perigee and the ellipticity are known exactly. Then the orbit can be represented in the $x-y$ plane, with the angle of perigee at 0° , pointing to the positive x -axis.

There are three angles of mathematical interest in this setting to describe the position of the object along the orbit: the *eccentric anomaly* (E), the *mean anomaly* (M) and the *true anomaly* (T), where all three angles are measured from perigee. The true anomaly describes the actual angular position of the object, as measured from the center of the earth. The mean anomaly has constant derivative with respect to time as the object moves, and hence simplifies the mathematical development. The eccentric anomaly is an intermediate angle of no direct interest. The relation between the angles is given as follows in radians, where e is the ellipticity, $0 \leq e < 1$:

$$\tan \frac{1}{2}T = \sqrt{\frac{1+e}{1-e}} \tan \frac{1}{2}E,$$

$$M = E - e \sin E.$$

These mappings are bijective, so any one angle determines the other two. The calculations are all straightforward, except that a numerical iteration is needed to solve for E from M .

Initially all three angles are defined on the same interval $-\pi \leq E, M, T \leq \pi$. The angles agree at the midpoint and endpoints. That is, if $E = 0, \pi$ or $-\pi$, then M and T also equal to $0, \pi$ or $-\pi$, respectively. Further the identification between angles is symmetric about the origin. That is, if E

corresponds to M and T , then $-E$ corresponds to $-M$ and $-T$. Finally, by periodic extension, the mapping between the three angles can be extended to any interval $-\pi + 2\pi k \leq E, M, T \leq \pi + 2\pi k$, $k \in \mathbb{Z}$, and thus to the whole real line.

Use the notation $E = f_{M\text{-to-}E}(M, e)$ to describe the transformation between M and E and similar notation for the transformations between other pairs of angles. The main transformations of interest are $f_{M\text{-to-}T}$ and $f_{T\text{-to-}M}$. The function $f_{M\text{-to-}T}$ here plays the role of the function h in Section II B and takes an angle on the mean anomaly scale to an angle on the true anomaly scale. Fig. 1 shows a plot of T vs. M for $e = 0.7$. Notice the highly nonlinear behaviour.

The mean anomaly is the simplest angle mathematically and statistically because it changes at a constant rate in time:

$$\phi(t) = \phi(0) + tn,$$

where n is the mean motion. The actual angular position along the orbit is given by the true anomaly $\theta(t) = f_{M\text{-to-}T}(\phi(t))$.

For the purposes of this section, suppose that the initial mean anomaly $\phi(0)$ at time $t = 0$ is known exactly, but that the mean motion n has some Gaussian uncertainty, $n \sim N(\mu_n, \sigma_n^2)$. Then after some time t_1 , say, the mean anomaly has distribution

$$\phi(t_1) \sim N(\phi(0) + t_1\mu_n, t_1\sigma_n^2).$$

However, the observation is on the true anomaly scale

$$\theta_{\text{obs}} \sim N(\theta(t_1), \tau^2), \quad \theta(t_1) = f_{M\text{-to-}T}(\phi(t_1)).$$

Note that even if σ_n^2 is small, $\sigma^2 = t_1\sigma_n^2$ can still become large by considering a large propagation time t_1 . For the purposes of this paper suppose σ^2 is not too large in order to avoid winding number issues. In particular, restrict $\sigma = t_1^{1/2}\sigma_n$ to be substantially less than 360° so that θ_{obs} can be treated as a number unambiguously satisfying $|\theta_{\text{obs}} - \theta(t_1)| < 360^\circ$. In other words the number of whole orbits undergone is essentially known. The choices $\sigma = 25^\circ$ and $\sigma = 15^\circ$ are used in the examples below.

At the same time, the typical angles-only observations will be highly accurate. Three choices for τ are used in each example: (a) $\tau = 0^\circ$ for a perfect measurement, (b) $\tau = 5.5E - 04^\circ$ (equal

to 2 arc-seconds) for a realistic measurement error, and (c) $\tau = 2^\circ$ for a good but less accurate measurement.

For convenience suppose time is measured in orbits, so that $t = 1$ denotes the time needed for one complete orbit. Also, to help our intuition, measure angles in degrees. Finally note that estimating n is equivalent to estimating $\phi(t_1)$ in this setting. Let $\phi(t_1)$ here correspond to the state x in Section II A, with variance σ^2 , and let z_{obs} denote the observed true anomaly, with variance τ^2 . Thus the the state variable is the mean anomaly $x = \phi(t_1)$ lying on the signal scale, and the observation is the true anomaly $z_{\text{obs}} = \theta_{\text{obs}}$ lying on the measurement scale.

Here are two numerical examples to illustrate the pitfalls of the EKF, UKF and to demonstrate the benefits of the IEKF, IUKF, OCEKF and OCUKF. For both examples a high value of ellipticity is used, $e = 0.7$, so that the function $h = f_{\text{M-to-T}}$ is very nonlinear and the differences between the various filters stand out prominently. The parameters for each example are listed in Table 2 and highlighted in Figure 1. In this figure, the projection of the circles onto the horizontal axis gives the prior means μ_x for Examples 1 and 2, respectively; the projection of the squares onto the vertical axis gives the corresponding observations z_{obs} , and the projection of the squares onto the horizontal axis gives the corresponding values of $x_{\text{obs}} = h^{-1}(z_{\text{obs}})$.

For each example three choices are considered for the measurement standard error: (a) zero, $\tau = 0^\circ$, (b) “small”, $\tau = 5.5E - 04^\circ = 2$ arc seconds, and (c) “large”, $\tau = 2^\circ$. The posterior means and standard deviations for various filters are summarized in Table 3. The row labelled “Exact” in that table gives the exact moments from the true posterior distribution, as computed by numerical integration.

Example 1. Since $x_{\text{obs}} = 310^\circ = 260^\circ + 2 \times 25^\circ = \mu_x + 2\sigma$, the observation is mildly unusual but not infeasible under the prior distribution. However, the different filters produce wildly different results.

For all three choices of τ , the posterior means from the IEKF,IUKF, OCEKF and OCUKF filters are either identical or very close to each other and to the exact value. However, the EKF and UKF filters produce posterior means that are so different, they are essentially incompatible with the exact posterior distribution, The discrepancy becomes greater as τ gets smaller. Fig. 2) illustrates

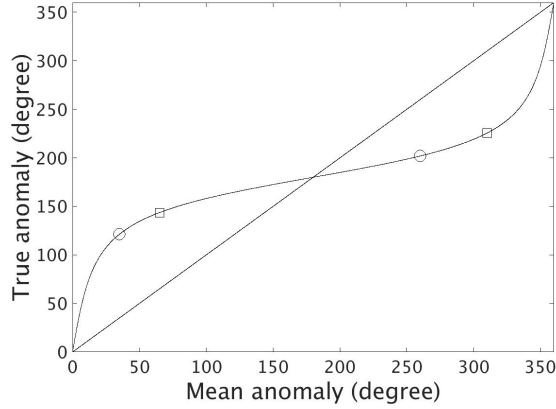


Fig. 1 True anomaly as a function of mean anomaly, for eccentricity $e = 0$ (diagonal straight line) and $e = 0.7$ (curved line). The marked points are defined in the text.

the issue in the least discrepant situation, case (c) with $\tau = 2^\circ$. The UKF posterior mean 323.5° is more than five standard deviations from the exact posterior mean 309.0° under the exact posterior distribution, $(323.5^\circ - 309.0^\circ)/2.8^\circ = 5.18$. The EKF is even worse.

Similarly, with a small exception, the posterior standard deviations from the IEKF, IUKF, OCEKF and OCUKF filters are either identical or very close to each other and to the exact value. The exception is the IUKF and OCUKF for $\tau = 0^\circ$. In this case the true posterior is a point mass at the posterior mean with posterior standard deviation 0° . However, the posterior standard deviation is overestimated by the IUKF and OCUKF filters. The reason is that these filters use differences rather than derivatives to deal with the nonlinearity. The problem would be ameliorated by using a smaller tuning parameter α in the construction of the unscented filters.

Example 2. As in Example 1, $x_{\text{obs}} = 65^\circ = 35^\circ + 2 \times 15^\circ = \mu_x + 2\sigma$, so again the observation is mildly unusual but not infeasible under the prior distribution. For the most part, the comparison between the different filters is very similar to the comparison in Example 1. The main difference is in the direction of the error. In Example 1 the posterior means for the EKF and UKF are *larger* than the true posterior mean, whereas in Example 2, the posterior means for the EKF and UKF are *smaller* than the true posterior mean. The reason is that h in Fig. 1 is *convex* at μ_x in Example 1 and it is *concave* at μ_x in Example 2.

Table 2 The prior mean μ_x and its standard deviation σ , plus the observation z_{obs} and its standard deviation τ , for **Examples 1 and 2**.

Example 1	Example 2
$\mu_x = 260^\circ$	$\mu_x = 35^\circ$
$\sigma = 25^\circ$	$\sigma = 15^\circ$
$z_{obs} = 225.5^\circ$	$z_{obs} = 143.6^\circ$
$x_{obs} = 310^\circ$	$x_{obs} = 65^\circ$
a: $\tau = 0^\circ$	
b: $\tau = 5.5E - 04^\circ$	
c: $\tau = 2^\circ$	

Table 3 Posterior means and standard deviations from various filters for **Examples 1(a, b, c) and 2(a, b, c)**.

KF/Example moment		1(a)	1(b)	1(c)	2(a)	2(b)	2(c)
Exact	mean	310.0 $^\circ$	309.9999 $^\circ$	309.0 $^\circ$	65.0 $^\circ$	64.9702 $^\circ$	63.5 $^\circ$
	s.d.	0 $^\circ$	7.7E-04 $^\circ$	2.8 $^\circ$	0 $^\circ$	1.1E-03 $^\circ$	3.5 $^\circ$
EKF	mean	329.8 $^\circ$	329.8584 $^\circ$	326.1 $^\circ$	55.0 $^\circ$	55.0748 $^\circ$	54.8 $^\circ$
	s.d.	0 $^\circ$	1.6E-03 $^\circ$	5.7 $^\circ$	0 $^\circ$	4.9E-04 $^\circ$	1.7 $^\circ$
UKF	mean	327.1 $^\circ$	325.2281 $^\circ$	323.5 $^\circ$	59.1 $^\circ$	59.1864 $^\circ$	58.9 $^\circ$
	s.d.	2E-03 $^\circ$	1.6E-03 $^\circ$	5.8 $^\circ$	4E-03 $^\circ$	5E-04 $^\circ$	1.8 $^\circ$
IEKF	mean	310.0 $^\circ$	309.9999 $^\circ$	309.3 $^\circ$	65 $^\circ$	64.9702 $^\circ$	63.2 $^\circ$
	s.d.	0 $^\circ$	7.7E-04 $^\circ$	2.8 $^\circ$	0 $^\circ$	1.1E-03 $^\circ$	3.5 $^\circ$
IUKF	mean	310.0 $^\circ$	309.9999 $^\circ$	309.3 $^\circ$	65 $^\circ$	64.9702 $^\circ$	63.2 $^\circ$
	s.d.	7E-03 $^\circ$	7.7E-04 $^\circ$	2.8 $^\circ$	2E-03 $^\circ$	1.1E-03 $^\circ$	3.5 $^\circ$
OCEKF	mean	310.0 $^\circ$	309.9999 $^\circ$	309.3 $^\circ$	65 $^\circ$	64.9702 $^\circ$	63.1 $^\circ$
	s.d.	0 $^\circ$	7.7E-04 $^\circ$	2.7 $^\circ$	0 $^\circ$	1.1E-03 $^\circ$	3.7 $^\circ$
OCUKF	mean	310.0 $^\circ$	309.9999 $^\circ$	309.3 $^\circ$	65 $^\circ$	64.9702 $^\circ$	63.2 $^\circ$
	s.d.	7E-03 $^\circ$	7.7E-04 $^\circ$	2.8 $^\circ$	2E-03 $^\circ$	1.2E-03 $^\circ$	3.7 $^\circ$

VI. Conclusions

Several conclusions can be made from these and other simulations.

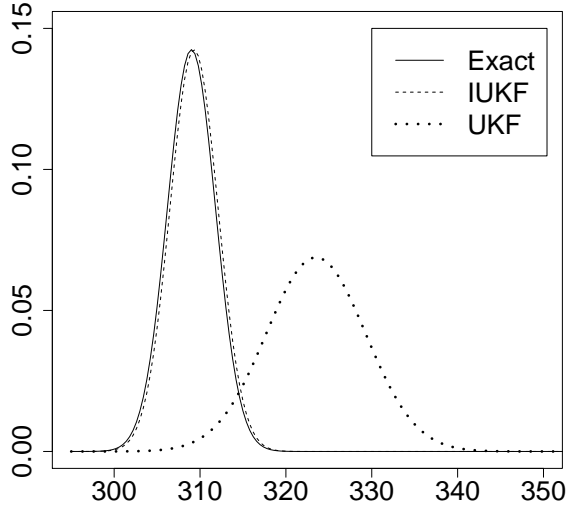


Fig. 2 Example 1(c). Exact posterior density together with the approximating Gaussian density from the IUKF and UKF filters. The exact posterior and the IUKF posterior densities are virtually indistinguishable.

- The EKF and UKF are standard methods to deal with nonlinear filtering problems; the UKF in particular is often used as an “off-the-shelf” method. However, when the nonlinearity is high and the observation variance τ^2 is small relative to the prior state variance σ^2 , these filters can perform very poorly.
- The development of the OCEKF and OCUKF in Sections II and III makes it clear why this behavior occurs. When τ^2 is small, it is better to base the Taylor series expansion at or near the observation, rather than at the prior mean.
- In terms of performance, the IEKF and OCEKF are very similar for the examples in this paper. Further, the posterior means and variances computed using these filters closely match the true posterior moments.
- The same statement is true for the IUKF and OCUKF, with one proviso. If τ^2 is very small or 0, the value of the posterior variance will depend noticeably on the tuning parameter α . To ensure the posterior variance from the filter is close to the true posterior variance, it is necessary to reduce the value of α below the default choice of $\alpha = 0.001$. Indeed, as pointed

out in Section II C, the limiting values of the IUKF and OCUKF as $\alpha \rightarrow 0$ are just the IEKF and OCEKF.

- One advantage of the OCEKF and OCUKF over the IEKF and the IUKF is that they do not require iteration.
- However, an advantage of the IEKF and the IUKF over the OCEKF and the OCUKF is that they are more widely applicable. In situations where τ^2 is not small relative to σ^2 (simulations not shown here), the posterior moments from the IEKF and IUKF can be closer to the true posterior moments.
- In the literature several other versions of the UKF and IUKF have been defined (e.g. [10–18]). However, in the setting of this paper, they are all identical to either the UKF or the IUKF.

Acknowledgment

This material is based upon work supported by the Air Force Office of Scientific Research, Air Force Materiel Command, USAF under Award No. FA9550-19-1-7000.

References

- [1] Pei, Y., Biswas, S., Fussell, D. S. and Pingali, K., *An Elementary Introduction to Kalman Filtering*. doi: arXiv:1710.04055.
- [2] Havlík, J. and Straka, O., *Performance evaluation of iterated extended Kalman filter with variable step-length*. Journal of Physics: Conference Series, IOP Publishing, Vol. 659, 2015, pp. 12–22. doi: 10.1088/1742-6596/659/1/012022.
- [3] Daum, F. E., *Extended Kalman Filters*. Encyclopedia of Systems and Control. Springer, London. doi: 10.1007/978-1-4471-5058-9.
- [4] Julier, S. J., *The scaled unscented transformation*. Proc. of the 2002 American Control Conference, November 2002, pp. 4555–4559. doi: 10.1109/ACC.2002.1025369.
- [5] Julier, S. J. and Uhlmann, J. K., *A New Extension of the Kalman Filter to Nonlinear Systems*. Proc. SPIE 3068, Signal Processing, Sensor Fusion, and Target Recognition VI, 1997. doi: 10.1117/12.280797.
- [6] Wan, E. A. and Merwe, R. V. D., *The unscented Kalman filter for nonlinear estimation*. Proc. of the IEEE 2000 Adaptive Systems for Signal Processing, Communications, and Control Symposium (Cat. No.00EX373), 2000, pp. 153–158. doi:10.1.1.361.9373.

- [7] Sibley, G., Sukhatme, G. and Matthies, L., *The Iterated Sigma Point Kalman Filter with Applications to Long Range Stereo*. Robotics: Science and Systems II, 2006, August 16-19. doi: 10.15607/RSS.2006.II.034.
- [8] Sabol, C. and Culp, R., *Improved angular observations in geosynchronous orbit determination*. Journal of Guidance, Control and Dynamics, Vol. 24, No. 1, January-February 2001, pp. 123–130. doi: 10.2514/2.4685.
- [9] Braun, C. V., Sharma, J. and Gaposchkin, E. M., *Space-based visible metric accuracy*. Journal of Guidance, Control and Dynamics, Vol. 23, No. 1, January-February 2000, pp. 175–181. doi: 10.2514/2.4508.
- [10] Zhu, J., Zheng, N., Yuan, Z., Zhang, Q., Zhang, X. and He, Y., *A SLAM algorithm based on the central difference Kalman filter*. IEEE Intelligent Vehicles Symposium, June 3-5, 2009. doi: 10.1109/IVS.2009.5164264.
- [11] Chaabane, M., Baklouti, I., Mansouri, M., Jaoua, N., Nounou, H., Nounou, M., Hamida, A. B. and Destain, F. M., *Nonlinear State and Parameter Estimation Using Iterated Sigma Point Kalman Filter: Comparative Studies*. Comparative Studies, Nonlinear Systems - Design, Analysis, Estimation and Control, IntechOpen, 2016. doi: 10.5772/63728.
- [12] Zhan, R. and Wan, J., *Iterated Unscented Kalman Filter for Passive Target Tracking*. IEEE Transactions on aerospace and electronic systems, Vol. 43, No. 3, July 2007. doi: 10.1109/TAES.2007.4383605.
- [13] Akram, M. A., Liu, P., Tahir, M. O., Ali, W. and Wang, Y., *A State Optimization Model Based on Kalman Filtering and Robust Estimation Theory for Fusion of Multi-Source Information in Highly Non-linear Systems*. Sensors, Vol. 19, No. 7, 2018. doi: 10.3390/s19071687.
- [14] Yadav, R., Date, A. and Bhaumik, P., *A New Method for Generating Sigma Points and Weights for Nonlinear Filtering*. IEEE Control Systems Letters, 2018. doi=10.1109/LCSYS.2018.2843184.
- [15] Ponomareva, K., Date, P. and Wang, Z., *A new unscented Kalman filter with higher order moment-matching*. Proceedings of the 19th Int. Symp. Mathematical Theory of Networks and Systems, Budapest, Hungary, 2010, pp. 1609–1613. doi=10.13140/2.1.1472.6089.
- [16] Yongfang, N. and Tao, Z., *Scaling parameters selection principle for the scaled unscented Kalman filter*. Journal of Systems Engineering and Electronics, Vol. 29, No. 3, June 2018, pp. 601–610. doi=10.21629/JSEE.2018.03.17.
- [17] Hu, G., Gao, S., Zhong, Y., Gao, B. and Subic, A., *Modified strong tracking unscented Kalman filter for nonlinear state estimation with process model uncertainty*. International Journal of Adaptive Control and Signal Processing, Vol. 29, No. 12, December 2015, pp. 1561–1577. doi=10.1002/acs.2572.
- [18] Raitoharju, M. and Piche, R., *On computational complexity reduction methods for Kalman filter exten-*

sions. doi: arXiv:1512.03077.